

AD-A141 577

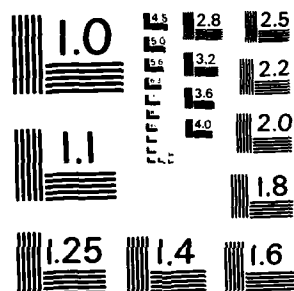
HIGH RESOLUTION MEASUREMENTS OF IMPURITY-INDUCED  
LOCALIZED VIBRATIONAL MO..(U) UNIVERSITY OF SOUTHERN  
CALIFORNIA LOS ANGELES ELECTRONIC SCIE.. W O SPITZER

UNCLASSIFIED

28 MAR 84 AFOSR-TR-84-0448 F33815-81-C-1406 F/O 20/12

11/  
NL

|  |  |  |  |  |  |  |  |  |  |  |  |  |                            |
|--|--|--|--|--|--|--|--|--|--|--|--|--|----------------------------|
|  |  |  |  |  |  |  |  |  |  |  |  |  |                            |
|  |  |  |  |  |  |  |  |  |  |  |  |  |                            |
|  |  |  |  |  |  |  |  |  |  |  |  |  |                            |
|  |  |  |  |  |  |  |  |  |  |  |  |  | END<br>DATE<br>7 84<br>DTN |



MICROCOPY RESOLUTION TEST CHART  
NATIONAL BUREAU OF STANDARDS-1963-A

UNCLASSIFIED

AD-A141 577

SECURITY CLASSIFICATION OF THIS PAGE

## REPORT DOCUMENTATION PAGE

|  |               |  |                    |                       |               |            |                  |                                      |             |           |  |  |  |  |  |
|--|---------------|--|--------------------|-----------------------|---------------|------------|------------------|--------------------------------------|-------------|-----------|--|--|--|--|--|
| 1a. REPORT SECURITY CLASSIFICATION<br><b>Unclassified</b>  |               | 1d. RESTRICTIVE MARKINGS<br><b>None</b>  |                    |                       |               |            |                  |                                      |             |           |  |  |  |  |  |
| 2a. SECURITY CLASSIFICATION AUTHORITY  |               | 3. DISTRIBUTION/AVAILABILITY OF REPORT<br><b>Approved for public release;<br/>distribution unlimited.</b>  |                    |                       |               |            |                  |                                      |             |           |  |  |  |  |  |
| 2b. DECLASSIFICATION/DOWNGRADING SCHEDULE  |               | 5. MONITORING ORGANIZATION REPORT NUMBER<br><b>AFOSR-TR- 34-0446</b>   |                    |                       |               |            |                  |                                      |             |           |  |  |  |  |  |
| 4. PERFORMING ORGANIZATION REPORT NUMBER<br><b>Final Report</b>  |               | 7a. NAME OF MONITORING ORGANIZATION<br><b>AFOSR/NE</b>   |                    |                       |               |            |                  |                                      |             |           |  |  |  |  |  |
| 6a. NAME OF PERFORMING ORGANIZATION<br><b>Electronic Sciences Lab.<br/>University of Southern Calif.</b>   |               | 7b. ADDRESS (City, State and ZIP Code)<br><b>Building 410<br/>Bolling AFB<br/>Washington, DC 20332</b>   |                    |                       |               |            |                  |                                      |             |           |  |  |  |  |  |
| 6b. OFFICE SYMBOL<br>(If applicable)   |               | 9. PROCUREMENT INSTRUMENT IDENTIFICATION NUMBER<br><b>Grant No. AFOSR-83-0092</b>  |                    |                       |               |            |                  |                                      |             |           |  |  |  |  |  |
| 6c. ADDRESS (City, State and ZIP Code)<br><b>University Park MC 0241<br/>University of Southern California<br/>Los Angeles, CA 90089-0241</b>  |               | 10. SOURCE OF FUNDING NOS.<br><table border="1"><tr><td>PROGRAM<br/>ELEMENT NO</td><td>PROJECT<br/>NO</td><td>TASK<br/>NO</td><td>WORK UNIT<br/>NO.</td></tr><tr><td><b>AFOSR<br/>Grant #<br/>83-0092</b></td><td><b>2306</b></td><td><b>B1</b></td><td></td></tr></table> |                    | PROGRAM<br>ELEMENT NO | PROJECT<br>NO | TASK<br>NO | WORK UNIT<br>NO. | <b>AFOSR<br/>Grant #<br/>83-0092</b> | <b>2306</b> | <b>B1</b> |  |  |  |  |  |
| PROGRAM<br>ELEMENT NO  | PROJECT<br>NO | TASK<br>NO   | WORK UNIT<br>NO.   |                       |               |            |                  |                                      |             |           |  |  |  |  |  |
| <b>AFOSR<br/>Grant #<br/>83-0092</b>   | <b>2306</b>   | <b>B1</b>  |                    |                       |               |            |                  |                                      |             |           |  |  |  |  |  |
| 11. TITLE (Include Security Classification) <b>High Resolution Measurements of Impurity-Induced Localized Vibrational Modes in Semiconductors</b>  |               |  |                    |                       |               |            |                  |                                      |             |           |  |  |  |  |  |
| 12. PERSONAL AUTHOR(S) <b>William G. Spitzer</b>   |               |  |                    |                       |               |            |                  |                                      |             |           |  |  |  |  |  |
| 13a. TYPE OF REPORT<br><b>Final Scientific Rept.</b>   |               | 13b. TIME COVERED<br><b>FROM 3/1/83 TO 2/29/84</b>   |                    |                       |               |            |                  |                                      |             |           |  |  |  |  |  |
| 14. DATE OF REPORT (Yr., Mo., Day)<br><b>84-3-26</b>   |               | 15. PAGE COUNT<br><b>35</b>  |                    |                       |               |            |                  |                                      |             |           |  |  |  |  |  |
| 16. SUPPLEMENTARY NOTATION   |               |  |                    |                       |               |            |                  |                                      |             |           |  |  |  |  |  |
| 17. COSATI CODES<br><table border="1"><tr><td>FIELD</td><td>GROUP</td><td>SUB. GR.</td></tr><tr><td></td><td></td><td></td></tr><tr><td></td><td></td><td></td></tr><tr><td></td><td></td><td></td></tr></table>   |               | FIELD  | GROUP              | SUB. GR.              |               |            |                  |                                      |             |           |  |  |  | 18. SUBJECT TERMS (Continue on reverse if necessary; and identify by block number) |  |
| FIELD  | GROUP         | SUB. GR.   |                    |                       |               |            |                  |                                      |             |           |  |  |  |  |  |
|  |               |  |                    |                       |               |            |                  |                                      |             |           |  |  |  |  |  |
|  |               |  |                    |                       |               |            |                  |                                      |             |           |  |  |  |  |  |
|  |               |  |                    |                       |               |            |                  |                                      |             |           |  |  |  |  |  |
| 19. ABSTRACT (Continue on reverse if necessary and identify by block number)<br><p>The recent measurements and study of the carbon-induced localized vibrational mode (LVM) in GaAs have demonstrated that nearest neighbor isotopic frequency shifts can be observed if one uses the high resolution capability of a Fourier transform infrared (FTIR) spectrometer. One major importance of such measurements lies in the use of the shifts to determine the impurity site and the formation of complexes such as dimers. This feature has been used by the author and W. M. Theis in a detailed study of the LVM infrared absorption of Si-doped GaAs. Samples electrically compensated by electron irradiation and by Li saturation were used in the study. Bands due to Si<sub>Ca</sub>, Si<sub>As</sub>, Si<sub>Ca</sub>-Si<sub>As</sub>, Li<sub>Ca</sub>, and Si<sub>As</sub>-As<sub>Ca</sub> (or V<sub>Ca</sub>) were studied in high resolution. In several cases the structures observed in the high resolution measurements were compared with model calculations with generally satisfactory results.</p> <p><b>DTIC FILE COPY</b></p> <p>*Avionics Laboratory at Wright Patterson AFB</p> |               |  |                    |                       |               |            |                  |                                      |             |           |  |  |  |  |  |
| 20. DISTRIBUTION/AVAILABILITY OF ABSTRACT<br><b>UNCLASSIFIED/UNLIMITED <input checked="" type="checkbox"/> SAME AS RPT. <input type="checkbox"/> DTIC USERS <input type="checkbox"/></b>   |               | 21. ABSTRACT SECURITY CLASSIFICATION<br><b>unclassified</b>  |                    |                       |               |            |                  |                                      |             |           |  |  |  |  |  |
| 22a. NAME OF RESPONSIBLE INDIVIDUAL  |               | 22b. TELEPHONE NUMBER<br>(Include Area Code)   | 22c. OFFICE SYMBOL |                       |               |            |                  |                                      |             |           |  |  |  |  |  |

DD FORM 1473, 83 APR

EDITION OF 1 JAN 73 IS OBSOLETE.

UNCLASSIFIED  
SECURITY CLASSIFICATION OF THIS PAGE

AFOSR-TR. 84-0446

FINAL REPORT

High Resolution Measurements of Impurity-Induced  
Localized Vibrational Modes in Semiconductors

by

William G. Spitzer

Electronic Sciences Laboratory  
University of Southern California

under

Grant #AFOSR-83-0092

From: 3/1/83  
To: 2/29/84

Report Date: 3/26/84

|                    |                                     |
|--------------------|-------------------------------------|
| Accession For      |                                     |
| NTIS GRA&I         | <input checked="" type="checkbox"/> |
| DTIC TAB           | <input type="checkbox"/>            |
| Unannounced        | <input type="checkbox"/>            |
| Justification      |                                     |
| By                 |                                     |
| Distribution/      |                                     |
| Availability Codes |                                     |
| Dist               | Avail and/or<br>Special             |
| A-1                |                                     |



Approved for public release;  
distribution unlimited.

# Abstract

The recent measurements and study of the carbon-induced localized vibrational mode (LVM) in GaAs have demonstrated that nearest neighbor isotopic frequency shifts can be observed if one uses the high resolution capability of a Fourier transform infrared (FTR) spectrometer. One major importance of such measurements lies in the use of the shifts to determine the impurity site and the formation of complexes such as dimers. This feature has been used by the author and W. M. Theis\* in a detailed study of the LVM infrared absorption of Si-doped GaAs. Samples electrically compensated by electron irradiation and by Li saturation were used in the study. Bands due to  $\text{Si}_{\text{Ga}}$ ,  $\text{Si}_{\text{As}}$ ,  $\text{Si}_{\text{Ga}}\text{-Si}_{\text{As}}$ ,  $^7\text{Li}_{\text{Ga}}$ , and  $\text{Si}_{\text{As}}\text{-As}_{\text{Ga}}$  (or  $\text{V}_{\text{Ga}}$ ) were studied in high resolution. In several cases the structures observed in the high resolution measurements were compared with model calculations with generally satisfactory results.

AIR FORCE OFFICE OF SCIENTIFIC RESEARCH (AFOSR)  
NOTICE OF RESEARCH RESULTS  
This report is the property of the Air Force Office of Scientific Research  
Approved for public release; distribution is unlimited.  
DISTRIBUTION STATEMENT  
MATTHEW J. KLEIN  
Chief, Technical Information Division

\* Avionics Laboratory at Wright Patterson AFB

## Report

### Introduction:

This report covers a one year period, 3/1/83 to 2/29/84, during which the author was working cooperatively with W. M. Theis, C. W. Litton, and K. K. Bajaj, all at the Avionics Laboratory at Wright Patterson Air Force Base. The purpose of the work was to exploit earlier observations of the affect of the change in mass of different nearest neighbors (isotopic change) on the frequency of localized vibrational modes induced by impurities in a crystalline lattice. The earlier observations of carbon in gallium arsenide, GaAs:C, were reviewed in the proposal for this project and will not be reviewed again here.

This report will detail some extensive measurements and interpretation of the LVM observed in GaAs:Si. Some of the <sup>samples</sup> and their electrical compensation were prepared for earlier low resolution studies in the author's laboratory. The samples were measured by W. M. Theis with a Nicolet Fourier transform spectrometer which has a maximum possible resolution of  $0.06 \text{ cm}^{-1}$ . The results of this study have been used to prepare a manuscript which is currently under review by the Journal of Applied Physics. A copy of the complete manuscript forms the body of this report as it describes in detail the work done in this contract period.

High Resolution Measurements of Localized Vibrational Mode Infrared  
Absorption of Si-Doped GaAs

W. M. Theis

University Research Center, Wright State University, Dayton, OH 45435

W. G. Spitzer

Departments of Materials Science and Physics,  
University of Southern California, Los Angeles, CA 90089-0241

(Received

### ABSTRACT

The infrared absorption due to excitation of localized vibrational modes (LVM) involving Si impurities in GaAs was measured at 80 K under high resolution conditions for  $1 \times 10^{18} \text{ cm}^{-3} \leq [\text{Si}] \leq 5 \times 10^{19} \text{ cm}^{-3}$ . Electrical compensation by Li diffusion or electron irradiation resulted in no observable differences in peak positions or linewidths for those LVM identified as  $\text{Si}_{\text{Ga}}$ ,  $\text{Si}_{\text{As}}$ , and pair absorptions. These modes (including the individual lines composing the  $\text{Si}_{\text{As}}$  LVM) had intrinsic linewidths of  $0.4 \text{ cm}^{-1}$  which broadened as  $[\text{Si}]$  increased. In electron irradiated materials, an absorption band with major peaks at 366.63, 368.31, 369.53, and 370.7  $\text{cm}^{-1}$  was seen to shift to lower energies by  $9.9 \text{ cm}^{-1}$  when  $^{28}\text{Si}$  was replaced with  $^{30}\text{Si}$ . Arguments are presented to suggest that the 366.63  $\text{cm}^{-1}$  peak may be due to  $\text{Si}_{\text{As}}$  paired with a nearest neighbor native defect such as  $\text{As}_{\text{Ga}}$  or a Ga vacancy. In Li compensated material, the isolated  $^{7}\text{Li}_{\text{Ga}}$  LVM was seen for the first time at 449.64  $\text{cm}^{-1}$  as well as several additional unidentified absorptions. The two bands due to  $^{28}\text{Si}_{\text{Ga}}-^{28}\text{Si}_{\text{As}}$  have asymmetrically broadened lines which are attributed to various configurations of nearest neighbor Ga isotopes in the host lattice and the observations are compared to model calculations. Finally, the band associated with  $^{28}\text{Si}_{\text{Ga}}-^{30}\text{Si}_{\text{As}}$  and  $^{30}\text{Si}_{\text{Ga}}-^{28}\text{Si}_{\text{As}}$  pairs were resolved into a doublet with peaks at 455.80 and 457.01  $\text{cm}^{-1}$ , respectively.



## 1) Introduction

There have been a number of studies<sup>(1-5)</sup> of the infrared absorption associated with the excitation of localized vibrational modes (LVM) in Si-doped GaAs. One of the primary reasons for the interest in this system, aside from the technological importance of the material, is the well-known amphoteric behavior of Si as an impurity in GaAs. There is a considerable body of evidence that Si not only forms shallow donors when substitutional on the Ga sublattice,  $\text{Si}_{\text{Ga}}$ , and acceptors when on the As sublattice,  $\text{Si}_{\text{As}}$ , but also enters into a number of complexes particularly when other impurities are present. The distribution of Si among the various point defects depends upon a number of factors which include the concentration of Si and the other impurities as well as the temperature of growth and of any subsequent thermal annealing. Localized vibrational mode infrared absorption bands are one of the experimental methods that have been used to identify and to study the Si-related defects. In some cases absorption cross sections have been correlated with measured impurity concentrations.

All of the previous infrared studies have involved the use of standard "commercial type" grating spectrometers in which the typical spectral resolution is at best  $\Delta\bar{\nu} = 0.5 \text{ cm}^{-1}$  and frequently close to  $1.0 \text{ cm}^{-1}$  for the spectral range of interest, i.e.  $300 \text{ cm}^{-1}$  to  $500 \text{ cm}^{-1}$ . In the present study we have measured the transmission of a number of Si-doped GaAs samples having different Si concentrations by using a Fourier transform infrared (FTIR) spectrometer under the highest resolution attainable with the instrument, i.e.  $\Delta\bar{\nu} = 0.06 \text{ cm}^{-1}$ . As is frequently the case when a significant increase in the resolution of an instrumental probe is achieved, several new features are observed and conclusions drawn from the earlier, low resolution data can be more rigorously tested and in some cases put on much firmer ground.

All of the samples used here as well as those of the previous LVM studies had to be electrically compensated in order to remove the large free carrier concentration and hence free carrier absorption in the infrared. The compensation methods most frequently employed are either electron irradiation or saturation diffusion of Li, both of which are used here. In all cases the measured linewidths are large compared to the instrumental resolution. The peak frequencies and line widths of the absorption bands can be determined very accurately thereby critically testing the prior hypothesis that certain defect LVM are independent of the nature of the compensating species and are therefore characteristic of the defects present in the original, pre-compensated samples. The high resolution measurements also show that all of the absorption bands fall into two general categories with respect to linewidths and the distinction between the two groups can be attributed<sup>(6,7)</sup> to a nearest neighbor (nn) isotopic broadening effect. For those cases in which the nn effect is present, we have one band where the effect produces structure which is largely resolved while for another pair of bands it causes asymmetric broadening. The mode due to  $\text{Li}_{\text{Ga}}$  which is unpaired with any other impurity is observed for the first time and a simple perturbation argument indicates that the observed frequency is close to that expected from ion pairs containing  $\text{Li}_{\text{Ga}}$ . The linewidth is essentially the same as that for a  $\text{Si}_{\text{Ga}}$  which also has four As nearest neighbors. A number of new bands are observed to occur, several in some samples and not in others. Although there is some speculation concerning a few of these bands, their origin remains unexplained.

## II) Background

There have been a number of LVM studies of Si-doped GaAs and some of the more recent papers summarize most of the earlier work.<sup>(1-7)</sup> For our present purposes it will suffice to review briefly the methods of sample compensation,

the observed LVM frequencies and the basis of the assignments to particular point defects.

When heavily-doped GaAs:Si is grown from a nearly-stoichiometric melt, it is always n-type, although the carrier density may depend upon the procedure employed for the "cool-down" from the growth temperature.<sup>(1)</sup> In order to observe the LVM absorption bands it is first necessary to reduce the free carrier density several orders of magnitude by introducing compensating defects. Simply cooling the material to freeze out the carriers will not suffice as the absorption associated with the photoionization of the  $\text{Si}_{\text{Ga}}$  shallow donor states will still obscure the LVM bands. One method of electrical compensation which has been used<sup>(2)</sup> is a saturation diffusion of Li (or Cu) at a temperature  $\geq 700^\circ\text{C}$ . With this method it has been well established that the diffusion process at elevated temperatures will cause the concentrations of some defect species to change as well as causing the introduction of some new defects involving Li ions. The changes become more pronounced as the diffusion temperature is raised. The second method of compensation involves high energy electron irradiation,<sup>(5)</sup> i.e. 1-2 MeV electrons for samples approximately 0.5 mm thick. The samples are cooled during the irradiation and evidence indicates that this method produces much less change in the pre-compensation defect concentrations than the Li diffusion.

Table I gives the previously reported frequencies, linewidths, and defect identification<sup>(1-5)</sup> of the principle absorption bands measured near 80 K for both methods of compensation. No attempt has been made in the table to distinguish between the two compensation methods for bands attributed to  $\text{Si}_{\text{Ga}}$ ,  $\text{Si}_{\text{As}}$ , and  $\text{Si}_{\text{Ga}}\text{-Si}_{\text{As}}$  as the frequencies and band appearances were sufficiently similar for both cases that they were taken as the same. This similarity of

the frequency of some bands was used with the appearance of other bands with only one compensation method and with the isotope shifts<sup>(8)</sup> introduced when  $^{28}\text{Si} \rightarrow ^{30}\text{Si}$  and  $^7\text{Li} \rightarrow ^6\text{Li}$ , as a primary factor in the process of identifying the defects responsible for the modes. By using the electrical characteristics given in Table I one could predict the free carrier density  $n_e$  before compensation<sup>(3,9)</sup> for a large number of samples having a range of Si concentrations from about  $1 \times 10^{18}$  to  $5 \times 10^{19} \text{ cm}^{-3}$  and with  $1 \times 10^{18} \leq n_e \leq 1 \times 10^{19} \text{ cm}^{-3}$ .

The only prior high resolution infrared absorption measurements of GaAs are of the modes due to  $^{12}\text{C}_{\text{As}}$  and  $^{28}\text{Si}_{\text{As}}$  in doped material.<sup>(6,7)</sup> It was found that these two absorption bands each had a resolvable structure and the similarity in the structure suggested that a common mechanism was responsible. Previous lower resolution measurements<sup>(10)</sup> had only determined that the full width at half maximum of the absorption, FWHM, of  $^{28}\text{Si}_{\text{As}}$  was significantly greater than that for  $^{28}\text{Si}_{\text{Ga}}$ . Indeed when measured in high resolution it was found that the  $^{28}\text{Si}_{\text{Ga}}$  mode was a simple Lorentzian shape with a FWHM which was much less than that indicated in Table I. The explanation of the structure for the  $^{12}\text{C}_{\text{As}}$  and  $^{28}\text{Si}_{\text{As}}$  bands was the reduction in symmetry and small frequency shifts produced by the two different, naturally occurring Ga isotopes distributed in different ways over the four nn sites to the impurity. The frequency shifts come about because the LVM is not totally localized to the impurity and some of the kinetic energy is due to nn vibrational motion. The shift in frequency of the peak due to four  $^{69}\text{Ga}$  nn  $\rightarrow$  four  $^{71}\text{Ga}$  nn was in reasonable accord with that predicted from a one-dimensional linear chain defect model and an estimate of the relative strengths also appeared to be approximated by a simple valence force model when one takes the naturally occurring isotopic abundances of Ga into account, i.e.  $^{69}\text{Ga}$  (60.4%) and  $^{70}\text{Ga}$

(39.6%). Subsequently, Leigh and Newman<sup>(11)</sup> used a first order, degenerate perturbation treatment to show that the observed structure could be approximated by the calculated shifts if one increased the bend/stretch force constant ratio at the  $^{12}\text{C}$  impurity site. It was the prior observations of the structure in the  $\text{Si}_{\text{As}}$  absorption band and the much smaller FWHM values which in large part prompted the 80 K remeasurement of the entire LVM absorption spectrum for the GaAs:Si system under the present high resolution conditions.

### III) Experimental

The samples used for the present measurements were all taken from horizontal Bridgeman-grown ingots. In general, four different ranges of Si concentrations were used; i.e.  $[\text{Si}]$  about  $0.5$  to  $1 \times 10^{18} \text{ cm}^{-3}$ ,  $3$  to  $5 \times 10^{18} \text{ cm}^{-3}$ ,  $2$  to  $3 \times 10^{19} \text{ cm}^{-3}$ , and  $5 \times 10^{19} \text{ cm}^{-3}$ . The initial carrier densities ranged from  $5 \times 10^{17} \text{ cm}^{-3}$  to  $1 \times 10^{19} \text{ cm}^{-3}$ . The sample preparation and compensation techniques have all been described in considerable detail in previous studies<sup>(1-5)</sup> and the same procedures were used here. Whenever possible the same samples measured previously<sup>(1-3)</sup> were remeasured here.

The infrared measurements were made by using a Nicolet Fourier transform infrared spectrometer which was operated at its maximum possible resolution of  $0.06 \text{ cm}^{-1}$ . A carbon glowbar source, mylar beamsplitter, and Ge bolometer detector were used. The cryostat, which was operated at liquid nitrogen temperature, was equipped with KRS-5 windows. A "boxcar" or constant apodization function was employed when the Fourier transform was calculated so as not to degrade the resolution.

### IV) Experimental Results and Discussion

The infrared measurements are illustrated in Fig. 1 for a set of three samples. The three samples are: (1) an electron-irradiated sample with a  $[\text{Si}]$  approximately  $5 \times 10^{19} \text{ cm}^{-3}$  and an initial  $n_e = 8 \times 10^{18} \text{ cm}^{-3}$ ; (2) a  $^7\text{Li}$ -diffused

sample with  $[\text{Si}]$  approximately  $5 \times 10^{18} \text{ cm}^{-3}$  and an initial  $n_e = 2.4 \times 10^{18} \text{ cm}^{-3}$ ; and (3) a nonintentionally-doped, thick, vapor phase epitaxially (VPE) grown GaAs sample with total impurity concentration less than  $10^{14} \text{ cm}^{-3}$  and with the substrate removed. The sample thicknesses,  $x$ , are given in the figure caption and regions where the transmission becomes less than 1% and the absorption coefficient becomes unreliable are indicated in the figure. Figure 2 gives expanded views for regions where some of the Si and the Li absorption bands occur. The absorption spectrum of the non-doped VPE layer has been subtracted from the electron-irradiated and Li-diffused samples in order to remove the lattice absorption. Repeats of measurements, such as those in Figs. 1 and 2, often with several months between, are extremely reproducible.

A summary of the results from the high resolution measurements are given in Table II. There are several important differences between the results given here and those of Table I. The average frequency,  $\bar{\nu}$ , of band maxima are determined in almost all cases to  $0.01 \text{ cm}^{-1}$  with RMS deviations of typically  $0.04 \text{ cm}^{-1}$ . The  $\Delta \equiv \text{FWHM}$  is either  $\sim 0.40 \text{ cm}^{-1}$ , rising to  $\sim 0.8 \text{ cm}^{-1}$  for the most heavily Si-doped samples, or  $\geq 1.1 \text{ cm}^{-1}$ . Because of the sensitivity of the measurement of FWHM to assumptions of the background absorption which is frequently present even after subtraction of the pure sample lattice absorption, the values of FWHM are estimated to be reliable only to  $\pm 0.05 \text{ cm}^{-1}$ . The high signal to noise ratio allows one to make meaningful absorption band measurements for very small changes in absorption coefficient--see some of the expanded curves in Fig. 2.

We will consider the results given in Table II for each defect species.

(i)  $\text{Si}_{\text{Ga}}$ :

There is considerable evidence in prior studies<sup>(1-5)</sup> that this defect is a shallow donor which has a point group symmetry  $T_d$  and should therefore have

one, triply degenerate LVM frequency. It is responsible for the absorption band listed in Table I near  $\bar{\nu} = 383.7 \text{ cm}^{-1}$  for  $^{28}\text{Si}_{\text{Ga}}$ ,  $378.5 \text{ cm}^{-1}$  for  $^{29}\text{Si}_{\text{Ga}}$  and  $373.4 \text{ cm}^{-1}$  for  $^{30}\text{Si}_{\text{Ga}}$ . In the high resolution measurements of electron-compensated material it is observed that there is no significant shift in any of these peak frequencies for  $1 \times 10^{18} \text{ cm}^{-3} \leq [\text{Si}] \leq 5 \times 10^{19} \text{ cm}^{-3}$  although the line width, i.e.  $\Delta \approx \text{FWHM}$ , essentially doubles for this same  $[\text{Si}]$  concentration range increasing from  $\sim 0.4 \text{ cm}^{-1}$  to  $\sim 0.8 \text{ cm}^{-1}$ . It is also observed that the peak positions are indeed independent of the compensation method. The  $^7\text{Li}$ -compensated samples in Table II came primarily from the two lower  $[\text{Si}]$  groups, i.e. approximately  $1 \times 10^{18} \text{ cm}^{-3}$ , and only one sample of a next higher  $[\text{Si}]$ , with no significant concentration dependence of FWHM observed. The values of FWHM for  $^{29}\text{Si}_{\text{Ga}}$  and  $^{30}\text{Si}_{\text{Ga}}$  defects could not be measured in the  $^7\text{Li}$ -compensated cases because of the overlapping bands from the  $(^{28}\text{Si}_{\text{Ga}}-^7\text{Li}_{\text{Ga}})$  pair defect--see Table II. For the  $^{28}\text{Si}_{\text{Ga}}$  band, the FWHM values are also the same for the low  $[\text{Si}]$  samples for either compensation method. We therefore conclude that these absorption bands are indeed characteristic of  $\text{Si}_{\text{Ga}}$  defects without any observable interaction effects from either irradiation-induced defects or from  $^7\text{Li}$  impurities.

(ii)  $(^{28}\text{Si}_{\text{Ga}}-^7\text{Li})$  pairs and  $^7\text{Li}_{\text{Ga}}$ :

The (Si-Li) pair defect occurs of course, only in the  $^7\text{Li}$ -compensated material and has  $C_s$  symmetry. The  $\text{Si}_{\text{Ga}}$  and  $\text{Li}_{\text{Ga}}$  are presumed to be on second neighbor sites. The six LVM bands are attributed to three predominately Si modes and three almost totally Li modes as determined by the isotopic frequency shifts<sup>(5)</sup> when  $^7\text{Li} \rightarrow ^6\text{Li}$  and  $^{28}\text{Si} \rightarrow ^{30}\text{Si}$ . Each ion in the pair essentially vibrates with force constants due to the crystal and the other ion. Because of overlap with other bands, the  $^{28}\text{Si}$  mode at  $404.84 \text{ cm}^{-1}$  is the only one of the three Si modes for which FWHM could be measured and the FWHM

value is the same, within the  $0.05 \text{ cm}^{-1}$  uncertainty, as that for the  $^{28}\text{Si}_{\text{Ga}}$  defect. Moreover a simple perturbation expression, which has been used with some success in the past,<sup>(5)</sup>  $\bar{\nu}^2 = 1/3 \sum_{i=1}^3 \bar{\nu}_i^2$ , where  $\bar{\nu}_i$  are the frequencies where the degeneracy has been lifted and  $\bar{\nu}$  is the unperturbed frequency, gives a value for the  $^{28}\text{Si}_{\text{Ga}}$  mode of  $\bar{\nu} = 385.51 \text{ cm}^{-1}$  which is only  $1.8 \text{ cm}^{-1}$  from the measured frequency.

The  $^7\text{Li}$  modes of the  $\text{Si}_{\text{Ga}}\text{-Li}_{\text{Ga}}$  pair are at higher frequencies than the Si modes but, as noted in previous work,<sup>(5)</sup> at much lower frequencies than one would predict from an isotopic substitutional model. It is of interest to note that the FWHM values are approximately  $0.40 \text{ cm}^{-1}$ , essentially the same as that for the  $\text{Si}_{\text{Ga}}$  modes in the pair and the isolated  $\text{Si}_{\text{Ga}}$  defect. By analogy one might expect the frequency for the isolated  $\text{Li}_{\text{Ga}}$  species to be near  $\bar{\nu}^2 = 1/3 \sum_{i=1}^3 \bar{\nu}_i^2 = 446.49 \text{ cm}^{-1}$  and have a FWHM near  $0.40 \text{ cm}^{-1}$ . As is seen in Fig. 2 a line does occur at  $449.64 \text{ cm}^{-1}$  and does have a FWHM of approximately  $0.45 \text{ cm}^{-1}$ . We have observed that this band shifts to  $482.31 \text{ cm}^{-1}$  when  $^7\text{Li} \rightarrow ^6\text{Li}$  and that this is the same shift as observed for the other Li modes and almost the full shift expected if Li is the only vibrational species. This band does not occur in all  $^7\text{Li}$ -compensated samples and is not correlated with the intensities of the Li bands of the  $(\text{Si}_{\text{Ga}}\text{-Li}_{\text{Ga}})$  pairs. This defect mode has not been observed previously although it has been sought. Further support for the identity of this mode comes from some early lower resolution measurements<sup>(12)</sup> of the  $^7\text{Li}$  modes for the  $(\text{Te}_{\text{As}}\text{-}^7\text{Li}_{\text{Ga}})$  pairs produced by  $^7\text{Li}$ -compensation of Te-doped GaAs. The argument for the character of the modes is similar to that given for the  $(\text{Si}_{\text{Ga}}\text{-Li}_{\text{Ga}})$  defect discussed above except that in this case the heavy Te has no LVM and the impurities are nn producing a  $C_{3v}$  symmetry for the defect. As expected two LVM bands are observed, at  $475$  and  $391 \text{ cm}^{-1}$  for  $^7\text{Li}$  and at  $419$  and  $510 \text{ cm}^{-1}$  for  $^6\text{Li}$ . Again



using the perturbation expression, one has  $449 \text{ cm}^{-1}$  for  ${}^7\text{Li}_{\text{Ga}}$  and  $482 \text{ cm}^{-1}$  for  ${}^6\text{Li}_{\text{Ga}}$  compared to the measured  $449.64 \text{ cm}^{-1}$  and  $482.31 \text{ cm}^{-1}$ , respectively. We believe the closeness of the agreement is largely fortuitous.

(iii)  ${}^{28}\text{Si}_{\text{As}}$ :

All of the Si and Li defects considered in the discussions above involve impurities which are substitutionally incorporated on the Ga sublattice. Therefore the nearest neighbor (nn) atoms of the host lattice are all As and there is only one As isotope. When the  ${}^{28}\text{Si}_{\text{As}}$  acceptor defect is considered then the four nn atoms are Ga and there are two abundant naturally occurring Ga isotopes. Since one expects some participation of the nn atoms in a LVM vibrational motion, different isotopic arrangements can give small shifts in LVM frequencies. Five different isotopic combinations on the four nn sites can occur with point groups as follows: four  ${}^{69}\text{Ga}$  ( $T_d$ ); three  ${}^{69}\text{Ga}$ -one  ${}^{71}\text{Ga}$  ( $C_{3v}$ ); two  ${}^{69}\text{Ga}$ -two  ${}^{71}\text{Ga}$  ( $C_{2v}$ ); one  ${}^{69}\text{Ga}$ -three  ${}^{71}\text{Ga}$  ( $C_{3v}$ ); and four  ${}^{71}\text{Ga}$  ( $T_d$ ). The number of LVM frequencies expected for the  ${}^{28}\text{Si}_{\text{As}}$  defect for each Ga arrangement is 1, 2, 3, 2, and 1, respectively for a total of 9 frequencies, some of which are expected to be nearly degenerate. In the previous measurements<sup>(6,7)</sup> of the  ${}^{28}\text{Si}_{\text{As}}$  mode these nn isotope shifts were used with the isotopic abundances and a simple valence force model to explain the structure seen in this band--see Fig. 4 near  $398 \text{ cm}^{-1}$ . The experimental measurements of this band for a number of samples were also fitted by using Lorentzian functions<sup>(7)</sup> to represent the individual lines. For example, the observed band in the sample having a  $[\text{Si}]$  of approximately  $2 \times 10^{18} \text{ cm}^{-3}$  (the third heaviest doped in Fig. 3) was well fitted by three Lorentzian functions having frequencies of  $398.57$ ,  $397.96$  and  $397.44 \text{ cm}^{-1}$ . As expected these values are close to the observed peak frequencies listed in Table II. Of greater interest are the FWHM values which were treated as independent

parameters during the fit and were found to be 0.42, 0.57, and 0.46  $\text{cm}^{-1}$ , respectively--all close to the FWHM values for the modes for  $\text{Si}_{\text{Ga}}$  and  $\text{Li}_{\text{Ga}}$ , where the isotope effect is not present. The FWHM values obtained for fitting the heaviest doped sample in Fig. 3 ( $[\text{Si}]$  approximately  $5 \times 10^{19} \text{ cm}^{-3}$ ) were 0.88, 0.50, and 0.80  $\text{cm}^{-1}$  with the same peak frequencies (within  $\pm 0.5 \text{ cm}^{-1}$ ) which again closely follows the FWHM of the mode for  $\text{Si}_{\text{Ga}}$  in the high  $[\text{Si}]$  samples which was 0.80  $\text{cm}^{-1}$ . These data demonstrate that the increase in overall width for  $^{28}\text{Si}_{\text{As}}$  for samples of large  $[\text{Si}]$  is nearly identical to that for the  $\text{Si}_{\text{Ga}}$  bands. This increase in linewidth of the individual lines results in a degradation in the structure of the  $^{28}\text{Si}_{\text{As}}$  band as shown in Fig. 3. As indicated in the caption this figure also demonstrates that the form of the structure is not a function of the method of compensation. We therefore conclude that the individual absorption bands making up the  $^{28}\text{Si}_{\text{As}}$  composite band appear to be similar in width to the other Si and Li bands although the number of bands in the composite are uncertain. This conclusion is important when considering the next defect.

(iv) ( $^{28}\text{Si}_{\text{Ga}}\text{-}^{28}\text{Si}_{\text{As}}$ ) pairs:

In this pair defect it is assumed that the substitutional Ga and As positions are nn sites. If one ignores the nn Ga isotope effect then this defect has  $C_{3v}$  symmetry and the six LVM frequencies have four values, two of which are doubly degenerate modes. Only two absorption bands, one at 463.72  $\text{cm}^{-1}$  and the other at 393.05  $\text{cm}^{-1}$ , have been identified from previous work<sup>(1)</sup> as due to this defect--see Table II. At one time it was thought that the A band in Fig. 2 and Table II at 366.63  $\text{cm}^{-1}$  was a third of the four expected Si pair bands but a number of independent pieces of evidence indicated that this assignment was incorrect. There are several reasons for attributing the two bands mentioned above to a  $^{28}\text{Si}$  dimer defect, presumably  $^{28}\text{Si}_{\text{Ga}}\text{-}^{28}\text{Si}_{\text{As}}$ , but a

convincing observation<sup>(8)</sup> was that in samples doped with nearly equal parts  $^{28}\text{Si}$  and  $^{30}\text{Si}$ , one observes not only the  $^{28}\text{Si}_{\text{Ga}}-^{28}\text{Si}_{\text{As}}$  and  $^{30}\text{Si}_{\text{Ga}}-^{30}\text{Si}_{\text{As}}$  modes but also the previously unresolved  $^{28}\text{Si}_{\text{Ga}}-^{30}\text{Si}_{\text{As}}$  and  $^{30}\text{Si}_{\text{Ga}}-^{28}\text{Si}_{\text{As}}$  modes, approximately at the mid-frequency position. This observation was unambiguous for the  $463.72\text{ cm}^{-1}$  mode (then called  $464\text{ cm}^{-1}$ ) and suggested by the data for the  $393.05\text{ cm}^{-1}$  band. The absence of these features in the case of the  $366.6\text{ cm}^{-1}$  mode clearly demonstrated that it does not arise from Si pair defects and thus it will be treated in the next section. Further evidence<sup>(4)</sup> that the  $366.6\text{ cm}^{-1}$  absorption is not related to the Si pair defect is that the absorptions near  $367\text{ cm}^{-1}$  and those near  $369\text{ cm}^{-1}$  do not correlate in strength with one another as a function of irradiation and subsequent annealing nor do they appear to correlate to the known pair absorptions at  $393\text{ cm}^{-1}$  and  $464\text{ cm}^{-1}$ .

From the measurements of the two  $^{28}\text{Si}_{\text{Ga}}-^{28}\text{Si}_{\text{As}}$  bands summarized in Table II it is apparent for both the peak frequencies and linewidths that the modes are not influenced by the compensation method and therefore they are a property of the GaAs:Si system. From the discussion above it is apparent that there should be a nn  $\text{Ga}_{\text{Ga}}$  isotope effect on the pair bands because the coupled Si modes involve the vibrational motion of  $^{28}\text{Si}_{\text{As}}$  which has four nn of which three are  $\text{Ga}_{\text{Ga}}$  and one is  $\text{Si}_{\text{Ga}}$ . The nn isotope effect is also suggested by the large FWHM values given in Table II. Moreover the band near  $393\text{ cm}^{-1}$  as shown in Fig. 3 clearly does not have a simple Lorentzian lineshape but is the result of overlapping bands.

One can qualitatively predict the observed lines by employing some simple assumptions. The band near  $463.72\text{ cm}^{-1}$  is the higher frequency mode and has been attributed<sup>(4)</sup> to the singly-degenerate, axial Si stretching mode ( $A_1^+$ ). Assuming that there is random population of the 3 nn Ga sites by the two Ga

isotopes and that the absorption cross section is independent of Ga isotope then there should be four axial bands having relative, normalized absorption strengths of 0.220, 0.433, 0.284, and 0.062, where the band strengths are ordered in descending frequency and the normalization is  $\sum_{i=1}^4 \text{strengths}_i = 1.0$ . Since the four bands correspond to three  $^{69}\text{Ga}_{\text{Ga}}$ , two  $^{69}\text{Ga}_{\text{Ga}} + \text{one } ^{71}\text{Ga}_{\text{Ga}}$ , one  $^{69}\text{Ga}_{\text{Ga}} + \text{two } ^{71}\text{Ga}_{\text{Ga}}$  and three  $^{71}\text{Ga}_{\text{Ga}}$ , the frequencies intervals between each neighboring pair of the four frequencies should be almost identical. This predicts that there should be a slightly asymmetric broadening of the 463.72 band with a larger width on the low frequency side. Figure 4 shows an expanded view of this band with the lattice absorption and background absorption for a heavily-Si-doped sample, where the  $[\text{Si}]$  is approximately  $5 \times 10^{19} \text{ cm}^{-3}$ , the half-widths measured from the peak position are 0.75 and 0.62  $\text{cm}^{-1}$ , where the larger value is the low frequency one. The measurement was repeated for two other heavily-Si-doped samples with similar results although the half-width values show some variation. If we further assume that the FWHM for each mode is between 0.7 to 0.8  $\text{cm}^{-1}$  which is similar to the FWHM for both the  $^{28}\text{Si}_{\text{Ga}}$  and the individual bands making up the  $^{28}\text{Si}_{\text{As}}$  absorption in the most heavily doped samples, then one can attempt to fit the band shape of Fig. 4 with basically only one adjustable parameter which is the spacing between adjacent modes. In order to complete the fit one must also scale the total peak height and the net peak position in frequency although the latter parameters have no influence on band profile. As is seen in Fig. 4 a good fit is obtained with the following parameters: the predicted normalized strengths; adjacent mode spacing of 0.4  $\text{cm}^{-1}$ ; and FWHM = 0.7  $\text{cm}^{-1}$  for all four modes. While the fit is excellent and the values are close to the expected ones, it is certainly not unique. It does illustrate however,

that a good fit can be obtained when using assumptions dictated by the data for other bands.

A situation similar to the one just described exists for the  $393.05\text{ cm}^{-1}$  pair band of Fig. 4 except the asymmetry of the band is more obvious and the situation is a little more complicated. This band is presumed<sup>(4)</sup> to be due to the doubly-degenerate, out-of-phase modes which are transverse to the  $C_3$  symmetry axis--the  $\text{Si}_{\text{Ga}}\text{-Si}_{\text{As}}$  bond ( $E^+$ ). There are two modes for each type of Ga isotope arrangement and four types of arrangements. One of the two frequencies when only one Ga isotope is in the nn sites is nearly degenerate to the frequency when all are of the dominant Ga isotope with the other frequency shifted to a position between that for all  $^{69}\text{Ga}$  or all  $^{71}\text{Ga}$  isotopes. Once again, including the statistics gives strengths of 0.439, 0.217, 0.142, and 0.204 for nn being three  $^{71}\text{Ga}$ , two  $^{71}\text{Ga}$  + one  $^{69}\text{Ga}$ , one  $^{71}\text{Ga}$  + two  $^{69}\text{Ga}$ , and three  $^{69}\text{Ga}$ , respectively. Although the ordering of the central frequencies cannot be conclusively established from this argument, the measured band can be approximated by this combination of four modes but since there is no requirement that the mode spacings be equal in this case one has many adjustable parameters. The particular set of parameters used in Fig. 4 to approximate the  $393.05\text{ cm}^{-1}$  band include the predicted relative strengths with the central lines interchanged, a spacing of  $0.3\text{ cm}^{-1}$ , and a FWHM =  $0.75\text{ cm}^{-1}$ . Again the result appears reasonable but in the absence of well-resolved structure it is not conclusive. A more thorough treatment by Kleinert<sup>(13)</sup> employing Green's functions to predict the structure of the pair modes also predicts four distinguishable modes for the  $393\text{ cm}^{-1}$  absorption. It is likely that this predicted structure may never be resolved since calculated separations appear to be on the order of the line widths typical of samples with the smallest [Si] in this study which already are at such a concentration

as to make pair absorption measurements extremely difficult. Furthermore, the estimated total strength of the  $493.7\text{ cm}^{-1}$  band by this work to that of the  $393.1\text{ cm}^{-1}$  is 1:2 whereas the measured value is nearer 1:4.5 for most samples in this study. There is also a prediction that the  $E^-$  band would occur near  $375\text{ cm}^{-1}$  with the  $A_1^-$  in the optic band. If the  $E^-$  were even weakly infrared active, it would be expected to appear in the very heavily doped samples but no such line could be identified.

As stated earlier in this section, the  $^{28}\text{Si}_{\text{Ga}}-^{30}\text{Si}_{\text{As}}$  and  $^{30}\text{Si}_{\text{Ga}}-^{28}\text{Si}_{\text{As}}$  absorptions were not previously resolved.<sup>(8)</sup> One of the same samples used in that study was measured under high resolution conditions with the result as shown in Fig. 5. The positions of the peaks are  $455.80$  and  $457.01\text{ cm}^{-1}$  which are slightly different from the predicted values of  $456.4$  and  $456.9\text{ cm}^{-1}$  for  $^{28}\text{Si}_{\text{Ga}}-^{30}\text{Si}_{\text{As}}$  and  $^{30}\text{Si}_{\text{Ga}}-^{28}\text{Si}_{\text{As}}$ , respectively. Assuming equal absorption strengths for the two Si isotope configurations, the relative isotopic abundance,  $x$ , defined as  $[^{28}\text{Si}]/[^{28}\text{Si}]+[^{30}\text{Si}]$  may be found using a random distribution description for the  $463.7$ ,  $457.0$ ,  $455.8$ , and  $448.7\text{ cm}^{-1}$  lines which should be in the proportion  $x^2:x(1-x):(1-x)x:(1-x)^2$ . The measured absorption strengths of  $9.0\text{ cm}^{-2}:9.4\text{ cm}^{-2}:9.9\text{ cm}^{-2}:12.9\text{ cm}^{-2}$  yields an  $x$  value of  $0.47$  for this particular sample. When this sample was grown it was the intent to dope with  $x=0.50$  although any value within  $0.4 < x < 0.6$  would not have been surprising. The sample was compensated with  $^6\text{Li}$  which produced a mode which obscured the analogous structure for the  $393\text{ cm}^{-1}$  pair absorption, so it is not reported here.

(v) A, B, C, D, and E Bands of Table II:

In earlier measurements two Si-related absorption bands were observed near  $367.2\text{ cm}^{-1}$  and  $368.5\text{ cm}^{-1}$ --see Table I. The  $367.2\text{ cm}^{-1}$  band is the one previously thought to be a  $(^{28}\text{Si}_{\text{Ga}}-^{28}\text{Si}_{\text{As}})$  pair band but later attributed to

an undetermined Si related defect<sup>(3,4)</sup>. This band is observed in samples independent of the compensation method while the  $368.5\text{ cm}^{-1}$  was found only in electron irradiated samples. In the present measurements, the A, B, C, D, and E bands are all seen in the  $e^-$  compensated samples. It appears that the A band is the former  $367.2\text{ cm}^{-1}$ , and the B, C, and D bands were probably all part of the unresolved  $368.5\text{ cm}^{-1}$  band. It is unlikely that the D band is the B(1) center<sup>(14)</sup> which also occurs near  $371\text{ cm}^{-1}$  since it involves the presence of boron impurities not present in these samples. In the present measurements it is observed that the A band increases in strength more rapidly with [Si] in the electron irradiated samples than the other bands in this group and therefore, they are not due to the same defect species, a conclusion which is in accord with that made previously<sup>(3,4)</sup>. It was also suggested previously<sup>(1)</sup> from correlation studies of LVM band strengths with pre-compensation values of carrier densities that the A mode is related to a donor defect and the unresolved B, C, and D lines to an acceptor center. The E line was not previously observed.

Based on the early measurements, the same behavior for the A through E lines would be expected if  $^{28}\text{Si} + ^{30}\text{Si}$  and indeed this is the case. Since the number of samples doped only with the enriched  $^{30}\text{Si}$  isotope were limited, only two samples were available for study, one of which was compensated by  $^6\text{Li}$  diffusion and the other by electron irradiation. The line analogous to the A band in  $^{28}\text{Si}$ -doped samples, labelled A', occurred in both samples but the lines B' through E' appeared only in the electron-irradiated sample and not the  $^6\text{Li}$  compensated one which is the identical behavior as lines A through E. The positions of these modes were: (A')  $357.19\text{ cm}^{-1}$ , (B')  $358.41\text{ cm}^{-1}$ , (C')  $359.52\text{ cm}^{-1}$ , (D')  $360.5\text{ cm}^{-1}$ , and the E' line was present but too weak for accurate determination. This corresponds to an average shift of  $9.9\text{ cm}^{-1}$  for

each line in the structure which is near the expected isotopic value. Again, this points out the early erroneous identification<sup>(8)</sup> of the then-called 357.5  $\text{cm}^{-1}$  absorption as due to  $^{30}\text{Si}$  pair defects. Rather, this band, which is the A' mode, is due to a mechanism such as that to be described in this section.

There is now a considerable body of information available concerning the A band: (1) A  $^{28}\text{Si}$ -related defect complex is involved, probably with one  $^{28}\text{Si}$  per complex as deduced from Si isotopic shift measurements; (2) the defect is a donor<sup>(3)</sup> and contributes to the original  $n_e$  value implying that the center is present prior to compensation; (3) the band is present for electron-compensated, Li-compensated, and Cu-compensated samples implying the center involves a native defect which is not unique to a particular compensation technique and again suggests the defect exists prior to compensation (One Cu-compensated sample was measured and showed the A, B, and C lines. The D and E lines were too weak to be certain of their presence. These lines were not seen by Newman<sup>(5)</sup> when he studied Cu compensated samples.); (4) lastly, the large value of FWHM for the A band given in Table II suggests  $^{28}\text{Si}_{\text{As}}$  involvement. One can speculate on the possible defects which could satisfy all of these conditions. One possibility is a center involving nn pairing between the  $\text{Si}_{\text{As}}$  acceptor and an antisite defect to give a single donor in the form of  $(^{28}\text{Si}_{\text{As}} - \text{As}_{\text{Ga}})$  pairs. If one considers the evidence for the donor behavior as weak and disregards this condition, then  $(^{28}\text{Si}_{\text{As}} - V_{\text{Ga}})$  pairs would also be possible where  $V_{\text{Ga}}$  denotes a Ga vacancy.

The observation<sup>(4)</sup> that the strength of the absorptions near 367  $\text{cm}^{-1}$  decreases with extensive electron irradiation and increase greatly with annealing may be used to further speculate on the identity of these bands. The extensive electron irradiations may be assumed to form many  $V_{\text{Ga}}$  and  $V_{\text{As}}$  with the displaced Ga and As atoms becoming interstitials,  $\text{Ga}_i$  and  $\text{As}_i$ , which



may diffuse at lower temperatures than the  $V_{Ga}$  or  $V_{As}$ . If the A band were indeed  $^{28}Si_{As}-As_{Ga}$  then, as the irradiation increased, the band would decrease slightly whenever either member of the pair would be removed by the irradiation. This cannot account for the amount of decrease observed since the concentration of this center is small compared to  $Ga_{Ga}$  and  $As_{As}$  which are removed with equal probability as the center. Instead an argument involving the very mobile interstitials may be invoked. One such possibility is  $(^{28}Si_{As}-As_{Ga}) + Ga_i \rightarrow ^{28}Si_{As} + As_i$ . The defect  $^{28}Si_{As}-V_{Ga}$  should form more rapidly with increased irradiations since removal of any of the Ga neighbors near any  $^{28}Si_{As}$  (which are much more abundant than the A band) creates this defect. During annealing a site transfer of As such as  $(^{28}Si_{As}-V_{Ga}) + As_{As} \rightarrow (^{28}Si_{As}-As_{Ga}) + V_{As}$  with the  $V_{As}$  diffusing away would cause a much enhanced A band as compared to that present when the sample is barely compensated, i.e. the as-grown  $^{28}Si_{As}-As_{Ga}$  concentration. This view agrees with the observed behavior. On the other hand, if the A band were due to the  $^{28}Si_{As}-V_{Ga}$  defect, it has been pointed out that this line would be expected to grow with irradiation instead of having the observed decrease. One would need to argue that some migration and combinations such as  $(^{28}Si_{As}-V_{Ga}) + Ga_i \rightarrow ^{28}Si_{As}$  were occurring more rapidly during irradiation than  $(^{28}Si_{As}-V_{Ga})$  formation. Then as annealing occurred, the  $V_{Ga}$  must diffuse and preferentially pair with  $^{28}Si_{As}$  forming the very great quantities of  $^{28}Si_{As}-V_{Ga}$  necessary in order to agree with the annealing behavior. It must be noted that the irradiation and annealing behavior of the line at  $369\text{ cm}^{-1}$  increased with irradiation and decreased with annealing making it possible to speculate that it might be  $(^{28}Si_{As}-V_{Ga})$  with enhanced formation during irradiation and  $(^{28}Si_{As}-V_{Ga}) + As_{As} \rightarrow (^{28}Si_{As}-As_{Ga}) + V_{As}$  during annealing which would increase the  $^{28}Si_{As}-As_{Ga}$  line at its expense. Furthermore the  $369\text{ cm}^{-1}$  band was previously

found to be an acceptor<sup>(3)</sup>, not inconsistent with the defect being  $^{28}\text{Si}_{\text{As}}-\text{V}_{\text{Ga}}$ , particularly since it is absent in Li-compensated materials where there should be few  $\text{V}_{\text{Ga}}$ . At any rate, these models are largely speculative and the situation would need to be clarified by a careful irradiation and annealing investigation. Such a study is beyond the scope of the present paper.

More complicated defects could be proposed but are even more speculative. Even with the simple defects suggested above, there are difficulties with the models. One difficulty is to explain the low frequency of the  $366.63\text{ cm}^{-1}$  band relative to the  $^{28}\text{Si}_{\text{As}}$  band near  $398\text{ cm}^{-1}$ . A second problem is the apparent lack of any other related absorption band. The reduction of the frequency is a reason for choosing nn pairs involving a small ion such as  $\text{As}_{\text{Ga}}^{2+}$  or a vacancy next to the  $\text{Si}_{\text{As}}$ . This may allow the nn force constants for the  $\text{Si}_{\text{As}}$  to soften and reduce the LVM frequencies. Since the  $\text{C}_{3v}$  pair defects have axial symmetry the A band should be one of a pair of  $\text{Si}_{\text{As}}$  bands. From the measurements already discussed there is no other related band for  $\tilde{\nu} > 366.63\text{ cm}^{-1}$  and detailed inspection of the absorption for  $\tilde{\nu} < 366.63\text{ cm}^{-1}$  failed to reveal any related structure. It is possible that the other mode frequency is either very near or below the top of the continuous band mode spectrum near  $300\text{ cm}^{-1}$  and therefore not observed. The origins of the other lines, i.e. B, C, D, and E are unknown although they are observed in electron irradiated and in Cu-compensated material but not in Li-compensated samples.

#### (vi) Other LVM Bands:

In some of the thirteen samples measured for the present study, LVM bands were observed which are not listed in Table II since they were either (i) thought to be weak isotopic Si counterparts of the  $^{28}\text{Si}$  bands but were too weak to be identified with certainty, or (ii) due to known impurity

contaminants or (iii) totally unrelated to any other modes and present only in an occasional sample. In the first group are two weak bands observed near 388.3 and 387.2  $\text{cm}^{-1}$  and thought to be the two main peaks of the structure in the  $^{30}\text{Si}_{\text{As}}$  band. This identification was confirmed by measurements of a sample doped with  $^{30}\text{Si}$ . In the second category is a band near 361.55  $\text{cm}^{-1}$  which is due to  $\text{Al}_{\text{Ga}}$ . Another band between 582.1 to 582.7  $\text{cm}^{-1}$  is due to the  $\text{C}_{\text{As}}$  defect<sup>(6,7)</sup> with the Ga nn-induced structure. Bands at 364.03 and 420.91  $\text{cm}^{-1}$  in  $^7\text{Li}$ -diffused samples are known to be  $^7\text{Li}$ -native defect bands<sup>(15)</sup>. Furthermore, in all the  $^7\text{Li}$ -doped samples there appears an absorption at 408.4  $\text{cm}^{-1}$  which occurs very near a maximum in the background multiphonon absorption and would therefore not be resolvable when measured under lower resolutions--see Fig. 1. After subtraction of the background absorption in a high resolution measurement such as in Fig. 2 the existence and strength of this line is clearly demonstrated although its origin is presently unknown.

There are a number of bands which fall into the third category and they are listed since, in some cases, they are not weak. Their presence indicates that there are significant concentrations present of as yet unidentified impurities or other point defects. In all cases these modes occur in Li-compensated samples, however most of these samples were not cut from the same ingots which were used for the electron-irradiated samples. Two weak bands observed at 433.1 and 442.4  $\text{cm}^{-1}$  are known to be  $^7\text{Li}$  related as they shift to 464.5 and 474.3  $\text{cm}^{-1}$  when  $^6\text{Li}$  is used. The others are of unknown origin and are listed in Table III with comments.

#### V) Summary:

High resolution FTIR measurements at 80<sup>0</sup>K of the LVM absorption spectrum of GaAs:Si for  $1 \times 10^{18} \leq [\text{Si}] \leq 5 \times 10^{19} \text{cm}^{-3}$  have yielded the band positions, halfwidths and, in some cases, structure with much improved accuracy over

previous lower resolution measurements. These data permit one to improve the bases upon which the defects responsible for the LVM are identified. Table II in the text lists the frequencies, full halfwidths, and defects responsible for all identified bands which are related to  $^{28}\text{Si}$  and observed in samples compensated by electron irradiation or by  $^7\text{Li}$  saturation diffusion. In several cases the same frequencies and widths observed for both compensation methods supports the contention that the defects responsible for the LVM are unrelated to the compensating defects and are characteristic of the pre-compensated material. It is found that all defects involving Si on a Ga site (only) or  $^7\text{Li}$  on a Ga site have LVM bands with full halfwidths of  $\sim 0.4 \text{ cm}^{-1}$  in samples of  $[\text{Si}] \leq 5 \times 10^{18} \text{ cm}^{-3}$ . These defects include  $^{28}\text{Si}_{\text{Ga}}$ ,  $^{29}\text{Si}_{\text{Ga}}$ ,  $^7\text{Li}_{\text{Ga}}$ , and  $(^{28}\text{Si}_{\text{Ga}} - ^7\text{Li}_{\text{Ga}})$  pairs. The  $^7\text{Li}_{\text{Ga}}$  band is reported for the first time. Bands involving defects where  $^{28}\text{Si}_{\text{As}}$  is present have widths  $\geq 1.1 \text{ cm}^{-1}$  and these include  $^{28}\text{Si}_{\text{As}}$ ,  $(^{28}\text{Si}_{\text{Ga}} - ^{28}\text{Si}_{\text{As}})$  pairs, and a possible  $(^{28}\text{Si}_{\text{As}} - \text{native defect})$  pair. As demonstrated previously, the  $^{28}\text{Si}_{\text{As}}$  mode shows a clearly overlapping band structure and the two bands observed for  $(^{28}\text{Si}_{\text{Ga}} - ^{28}\text{Si}_{\text{As}})$  have asymmetrically broadened line shapes—one pronounced and the other only slight. Following previous arguments<sup>(6,7)</sup> the broad lines and structures are attributed to overlapping bands coming from frequency shifts produced by different distributions of the two Ga isotopes on the nearest neighbor positions to the  $\text{Si}_{\text{As}}$ . Since there is only one As isotope this effect is not present for  $\text{Si}_{\text{Ga}}$  or  $\text{Li}_{\text{Ga}}$  defects. It is shown that the  $\text{Si}_{\text{As}}$  linewidth of a band for any given Ga isotopic configuration is similar to that for the modes due to  $\text{Si}_{\text{Ga}}$  and  $\text{Li}_{\text{Ga}}$  defects. A number of other LVM absorption bands due to other known impurities or of unknown origin are noted.

## VI) Acknowledgments

The authors wish to express their appreciation to K. K. Bajaj, G. B. Norris, and C. W. Litton for helpful discussions; to J. E. Hoelscher for assistance in operating the spectrometers; and to D. E. Johnson for sample preparation. This work was performed under AFOSR Contracts F33615-81-C-1406 and AFOSR-83-0092.

### References

1. R. T. Chen and W. G. Spitzer, J. Electronic Mat. 10, 1085 (1981).
2. R. T. Chen and W. G. Spitzer, J. Electrochem. Soc. 127, 1607 (1980).
3. R. T. Chen, V. Rana, and W. G. Spitzer, J. Appl. Phys. 51, 1532 (1980).
4. M. R. Brozel, R. C. Newman, and B. Obzay, J. Phys. C. 12, L785 (1979).
5. For reviews and references to earlier work, see:  
R. C. Newman, Infrared Studies of Crystal Defects (Taylor and Francis, London) 1974; A. S. Barker, Jr. and A. J. Sievers, Rev. Mod. Phys. 47, Suppl. No. 2, S1 (1975); W. G. Spitzer, Festkorperprobleme XI edited by O. Madelung (Permagon, London) pp1-44, 1971.
6. W. M. Theis, K. K. Bajaj, C. W. Litton, and W. G. Spitzer, Appl. Phys. Lett. 41, 70 (1982).
7. W. M. Theis, K. K. Bajaj, C. W. Litton, and W. G. Spitzer, Physica 117B and 118B, 116 (1983).
8. P. C. Leung, J. Fredrickson, W. G. Spitzer, A. Kahan, and L. Bouthillette, J. Appl. Phys. 45, 1009 (1974).
9. K. Laithwaite and R. C. Newman, J. Phys. C. 9, 4503 (1976).
10. K. Laithwaite and R. C. Newman, Phil. Mag. 35, 1689 (1977).
11. R. S. Leigh and R. C. Newman, J. Phys. C: Sol. St. 15, L1045 (1982).
12. W. Hayes, Phys. Rev. 138, A1227 (1965); O. G. Lorimor and W. G. Spitzer, J. Appl. Phys. 38, 2713 (1967).
13. P. Kleinert, Phys. Stat. Sol.(b) 117, K91 (1983).
14. M. R. Brozel and R. C. Newman, J. Phys. C., Solid St. Phys. 11, 3135 (1978).
15. M. E. Leung and W. G. Spitzer, J. Phys. C. 6, 3223 (1973).

TABLE I: Previously Reported LVM Frequencies in Si-doped GaAs

| <u>Mode</u>         | <u>Linewidths</u>   | <u>Electrical</u> | <u>Impurity</u>    | <u>Defect</u>  |
|---------------------|---------------------|-------------------|--------------------|--|
| <u>Frequency</u>    | (FWHM)              | <u>Character</u>  |                    |  |
| (cm <sup>-1</sup> ) | (cm <sup>-1</sup> ) |                   |                    |  |
| 455                 | ~ 1.5-2.0           |                   | } <sup>7</sup> Li  | } <sup>28</sup> Si <sub>Ga</sub> - <sup>7</sup> Li <sub>Ga</sub> |
| 448                 | ~ 1.5-2.0           |                   |                    |  |
| 438                 | ~ 1.5-2.0           |                   |                    |  |
| 405                 | ~ 2.0               |                   | } <sup>28</sup> Si |  |
| 379                 | ~ 2.0               |                   |                    |  |
| 374                 | ~ 2.0               |                   |                    |  |
| 398.2               | ≥ 2.1               | acceptor          | <sup>28</sup> Si   | <sup>28</sup> Si <sub>As</sub>                                   |
| 383.7               | 1.4-1.5             | donor             | <sup>28</sup> Si   | <sup>28</sup> Si <sub>Ga</sub>                                   |
| 378.5               | -                   | donor             | <sup>29</sup> Si   | <sup>29</sup> Si <sub>Ga</sub>                                   |
| 373.4               | -                   | donor             | <sup>30</sup> Si   | <sup>30</sup> Si <sub>Ga</sub>                                   |
| 464.0               | ~ 2.0               |                   | } <sup>28</sup> Si | <sup>28</sup> Si <sub>Ga</sub> - <sup>28</sup> Si <sub>As</sub>  |
| 393.0               | ≥ 2.1               |                   |                    |  |
| 367.2               | ≥ 1.5               | donor             | <sup>28</sup> Si   | <sup>28</sup> Si + native defect                                 |
| 368.5               | ≥ 2.0               | acceptor          | <sup>28</sup> Si   | <sup>28</sup> Si + e <sup>-</sup> irradiation<br>produced defect |

Table II: LVM Frequencies and Full Widths at Half Maxima (FWHM) at 80 K

| Defect   | Electron-Compensated |                     |   |                           | <sup>7</sup> Li-Compensated |                     |   |                     |
|--|----------------------|---------------------|---|---------------------------|-----------------------------|---------------------|---|---------------------|
| Identification   | $\nu$                | RMS(a)              | N | $\Delta$ (c)              | $\nu$                       | RMS(a)              | N | $\Delta$ (c)        |
|  | (cm <sup>-1</sup> )  | (cm <sup>-1</sup> ) |   | (cm <sup>-1</sup> )       | (cm <sup>-1</sup> )         | (cm <sup>-1</sup> ) |   | (cm <sup>-1</sup> ) |
| <sup>28</sup> Si <sub>Ga</sub>   | 383.68               | 0.06                | 6 | 0.45                      | 383.69                      | 0.02                | 2 | 0.40                |
| <sup>29</sup> Si <sub>Ga</sub>   | 378.26               | 0.03                | 9 | 0.40(0.82) <sup>(b)</sup> | 378.22                      | 0.04                | 3 | -                   |
| <sup>30</sup> Si <sub>Ga</sub>   | 373.21               | 0.04                | 8 | 0.45(0.85)                | 373.20                      | 0.03                | 3 | -                   |
| <sup>28</sup> Si <sub>As</sub>   | 398.61               | 0.04                | 8 | 1.50(1.80)                | 398.63                      | 0.02                | 3 | 1.40                |
|  | 398.08               | 0.04                | 4 | 1.50(1.80)                | 398.07                      | 0.01                | 2 | 1.40                |
|  | 397.62               | 0.03                | 4 | 1.50(1.80)                | 397.49                      | 0.02                | 3 | 1.40                |
| <sup>28</sup> Si <sub>Ga</sub> - <sup>28</sup> Si <sub>As</sub>  | 463.72               | 0.08                | 6 | 1.10(1.50)                | 463.78                      | 0.02                | 3 | 1.10                |
|  | 393.05               | 0.05                | 8 | 1.50(1.70)                | 393.13                      | 0.03                | 3 | 1.50                |
| <sup>7</sup> Li <sub>Ga</sub>  |                      |                     |   |                           | 449.64                      | 0.04                | 2 | 0.45                |
| <sup>28</sup> Si <sub>Ga</sub><br>in<br>( <sup>28</sup> Si <sub>Ga</sub> - <sup>7</sup> Li <sub>Ga</sub> ) |                      |                     |   |                           | 404.84                      | 0.02                | 2 | 0.45                |
|  |                      |                     |   |                           | 378.19                      | 0.02                | 2 | -                   |
|  |                      |                     |   |                           | 372.72                      | 0.02                | 2 | -                   |
| <sup>7</sup> Li <sub>Ga</sub><br>in<br>( <sup>28</sup> Si <sub>Ga</sub> - <sup>7</sup> Li <sub>Ga</sub> )  |                      |                     |   |                           | 454.19                      | 0.02                | 2 | 0.40                |
|  |                      |                     |   |                           | 447.39                      | 0.08                | 2 | 0.40                |
|  |                      |                     |   |                           | 437.75                      | 0.02                | 2 | 0.40                |
| A  | 366.63               | 0.04                | 8 | 1.10(1.45)                | 366.65                      | -                   | 2 | (2.0)               |
| B  | 368.31               | 0.04                | 5 | -                         |                             |                     |   |                     |
| C  | 369.53               | 0.03                | 4 | -                         |                             |                     |   |                     |
| D  | 370.7                | 0.1                 | 4 | -                         |                             |                     |   |                     |
| E  | 375.8                | 0.1                 | 4 | -                         |                             |                     |   |                     |



FOOTNOTES TO TABLE II

(a)  $RMS = \left[ \frac{\sum (v - \bar{v})^2}{N} \right]^{1/2}$  where  $N$  = number of samples measured,  $\bar{v}$  is the

average of the measured peak frequencies.

(b) Values in ( ) are those measured for samples having highest [Si]'s. All others are low [Si] measurements.

(c)  $\Delta$  = bandwidth = full width at half maximum (FWHM)

TABLE III: ABSORPTION BANDS OF UNKNOWN ORIGIN

| <u>Frequency (at 80K)</u><br>( $\text{cm}^{-1}$ ) | <u>Number of Samples</u><br><u>in which observed</u> | <u>Comments</u>   |
|---|--|---|
| 433.1   | 1  | } $^7\text{Li}$ -related as also seen shifted in<br>frequency in one $^6\text{Li}$ -compensated sample  |
| 442.4   | 1  |   |
| 408.38  | 4  | FWHM = $0.45 \text{ cm}^{-1}$   |
| 335.5   | 1  | } Both in same sample. The $335.5 \text{ cm}^{-1}$ band<br>as strong as the $^{28}\text{Si}_{\text{Ga}}$ band and<br>much stronger than all other $^{28}\text{Si}$ -related<br>bands. |
| 328.65  | 1  |   |

### Figure Captions

FIG 1. Infrared absorption spectra at liquid nitrogen temperature for (1) an electron-irradiated sample with a  $[\text{Si}]$  approximately  $5 \times 10^{19} \text{ cm}^{-3}$ , thickness of 0.4 mm, (2) a  $^7\text{Li}$ -diffused sample with  $[\text{Si}]$  approximately  $5 \times 10^{18} \text{ cm}^{-3}$ , thickness of 1.2 mm, and (3) a nonintentionally-doped VPE sample with total impurity concentration less than  $10^{14} \text{ cm}^{-3}$ , thickness of 0.7 mm. Regions for which transmission fell below 1% which makes the absorption coefficient unreliable occur for values greater than the dashed line. See text for other details on samples and identity of absorption bands. Sample (2) in particular shows the carbon LVM at  $582 \text{ cm}^{-1}$ , the Al LVM at  $362 \text{ cm}^{-1}$ , and an unknown absorption at  $328.7 \text{ cm}^{-1}$ .

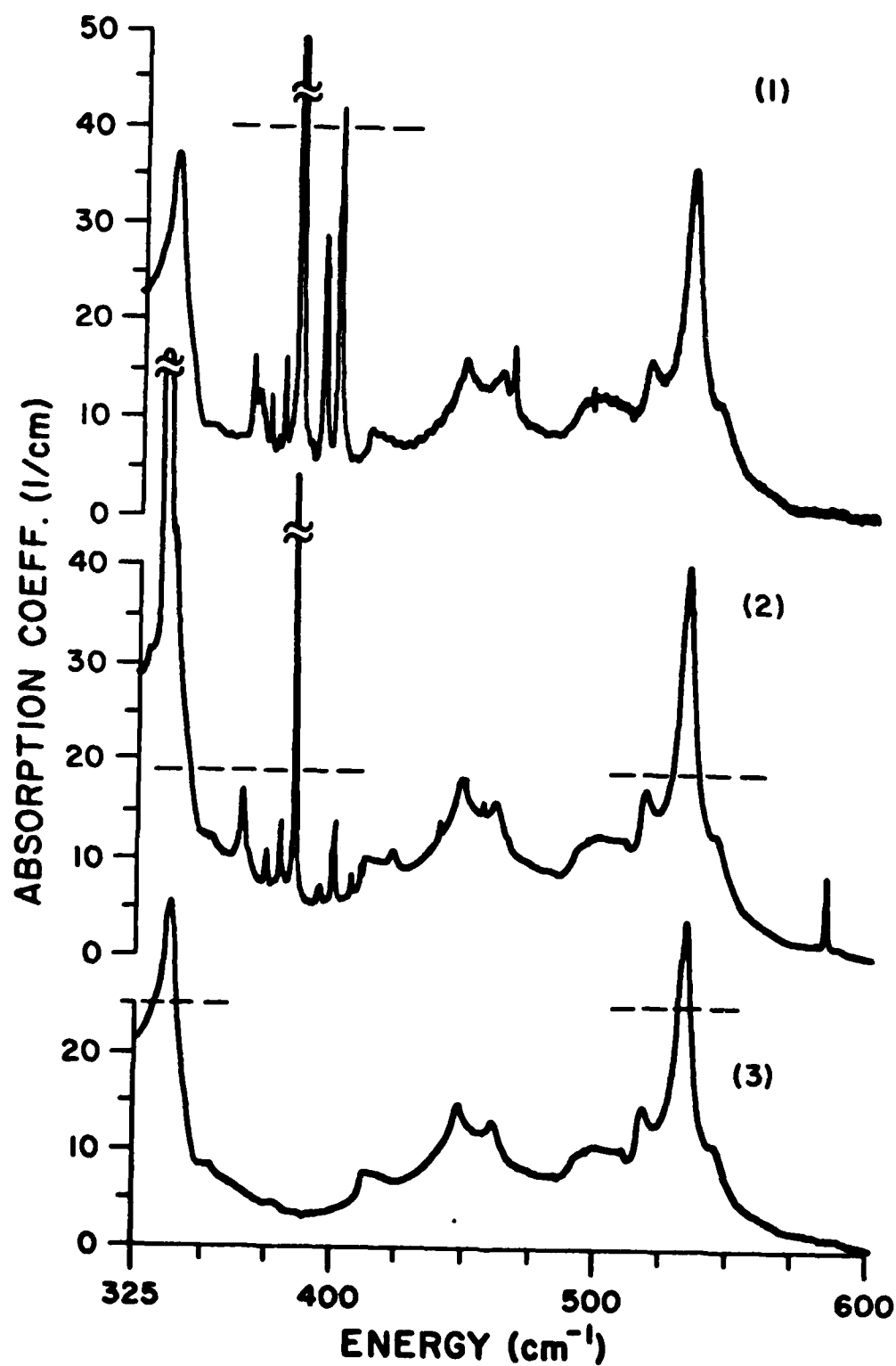
FIG 2. Infrared absorption spectra at liquid nitrogen temperature for samples (1) electron-irradiation compensated Si-doped sample and (2)  $^7\text{Li}$ -compensated sample both after subtraction of sample (3) the nonintentionally doped VPE sample to remove lattice absorptions. The cause of the residual background near the A band in sample (2) is the strong Al LVM at  $362 \text{ cm}^{-1}$  on whose shoulder the A band is located. The unidentified  $408.4 \text{ cm}^{-1}$  shows clearly in this sample after the subtraction is accomplished. See text for details on other bands.

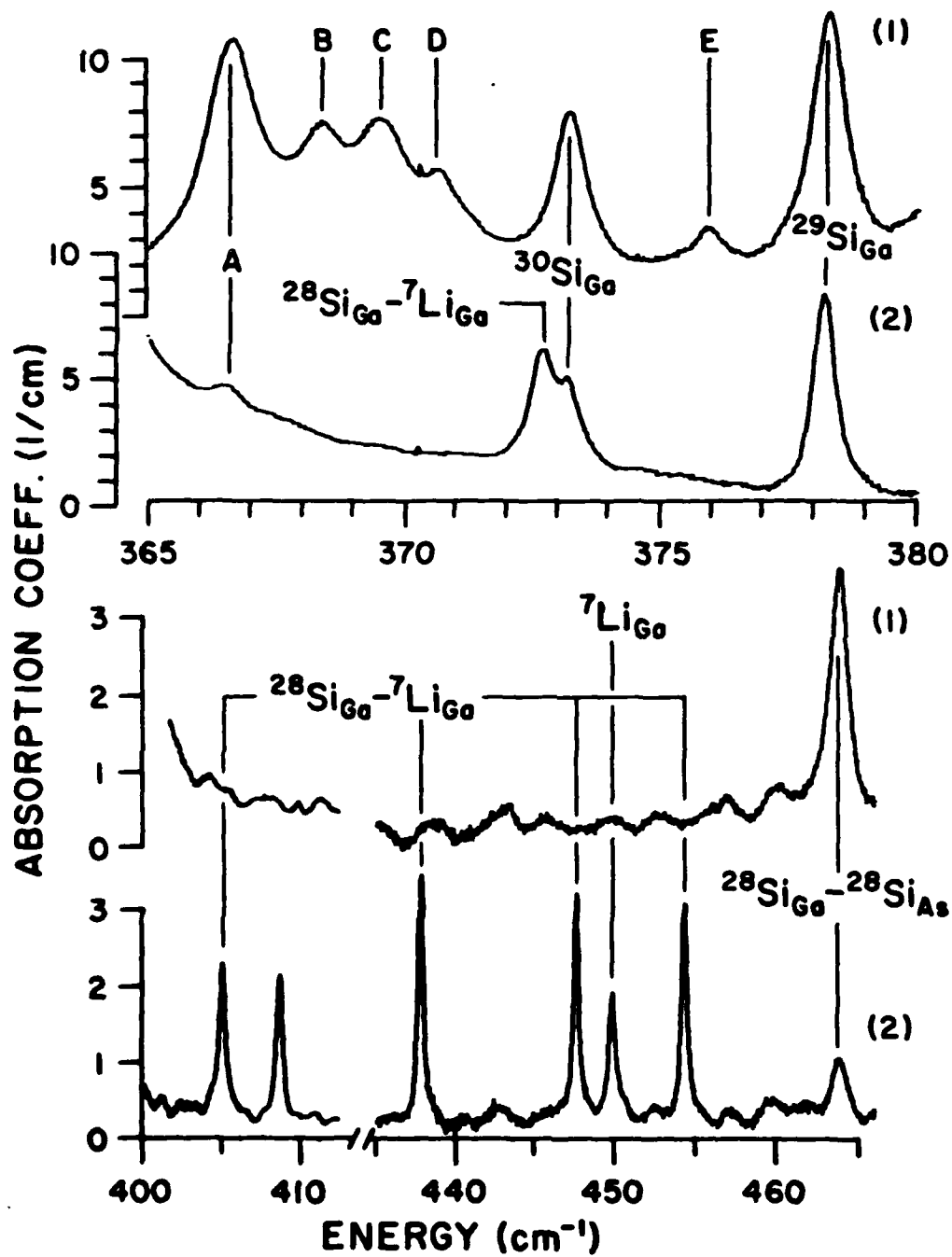
FIG 3. Infrared absorption spectra at liquid nitrogen temperature for the  $393 \text{ cm}^{-1}$  pair absorption and  $^{28}\text{Si}_{\text{As}}$  for the range of  $[\text{Si}]$  samples in this study. The two heaviest doped ( $[\text{Si}]$  approximately  $5 \times 10^{19}$  and  $3 \times 10^{19} \text{ cm}^{-3}$ , respectively) and lightest doped ( $[\text{Si}]$  approximately  $5 \times 10^{17} \text{ cm}^{-3}$ ) samples were compensated by electron irradiation with

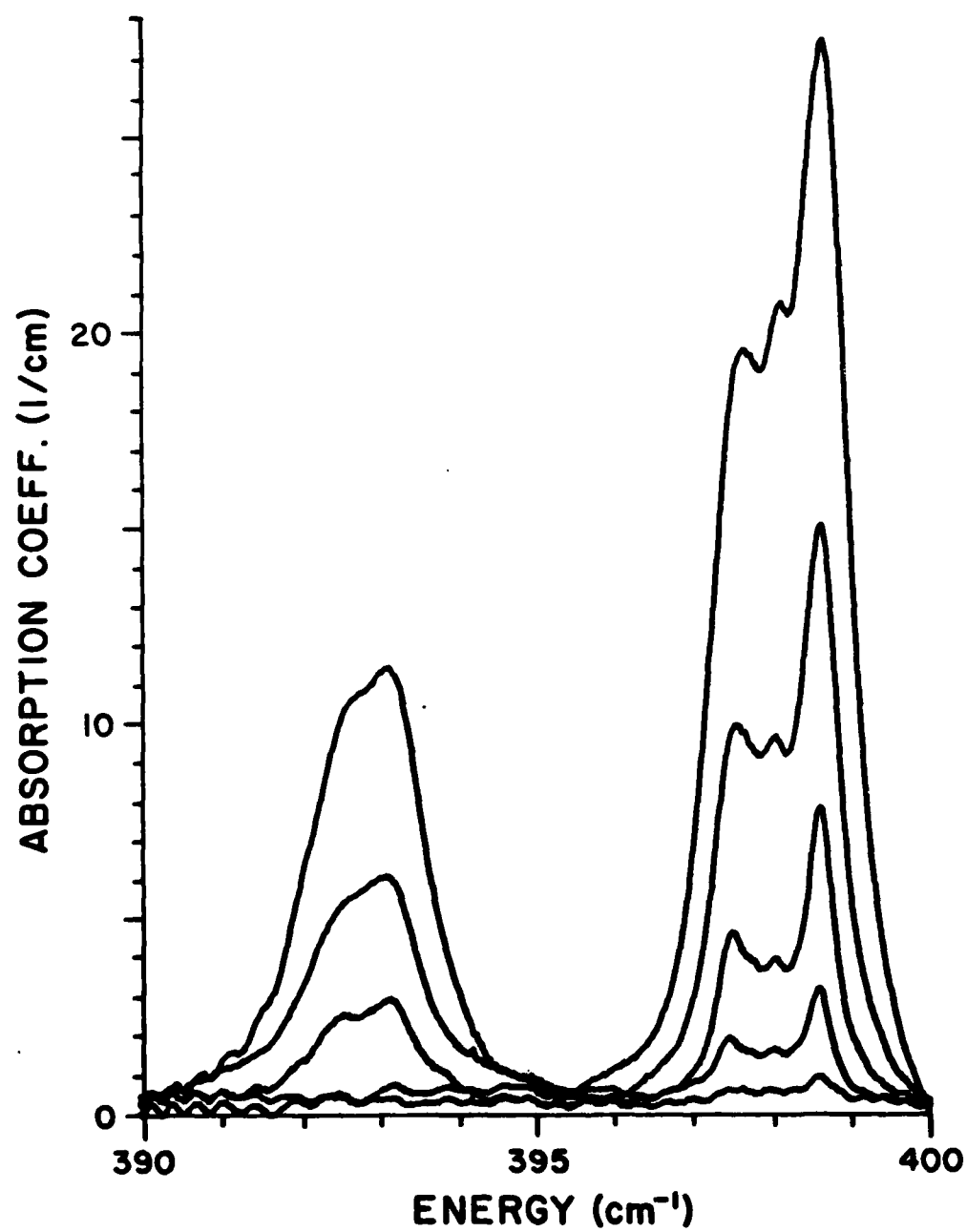
the third and fourth most heavily doped samples compensated by  $^7\text{Li}$  diffusion ( $[\text{Si}]$  approximately  $2 \times 10^{18}$  and  $1 \times 10^{18} \text{ cm}^{-3}$ , respectively).

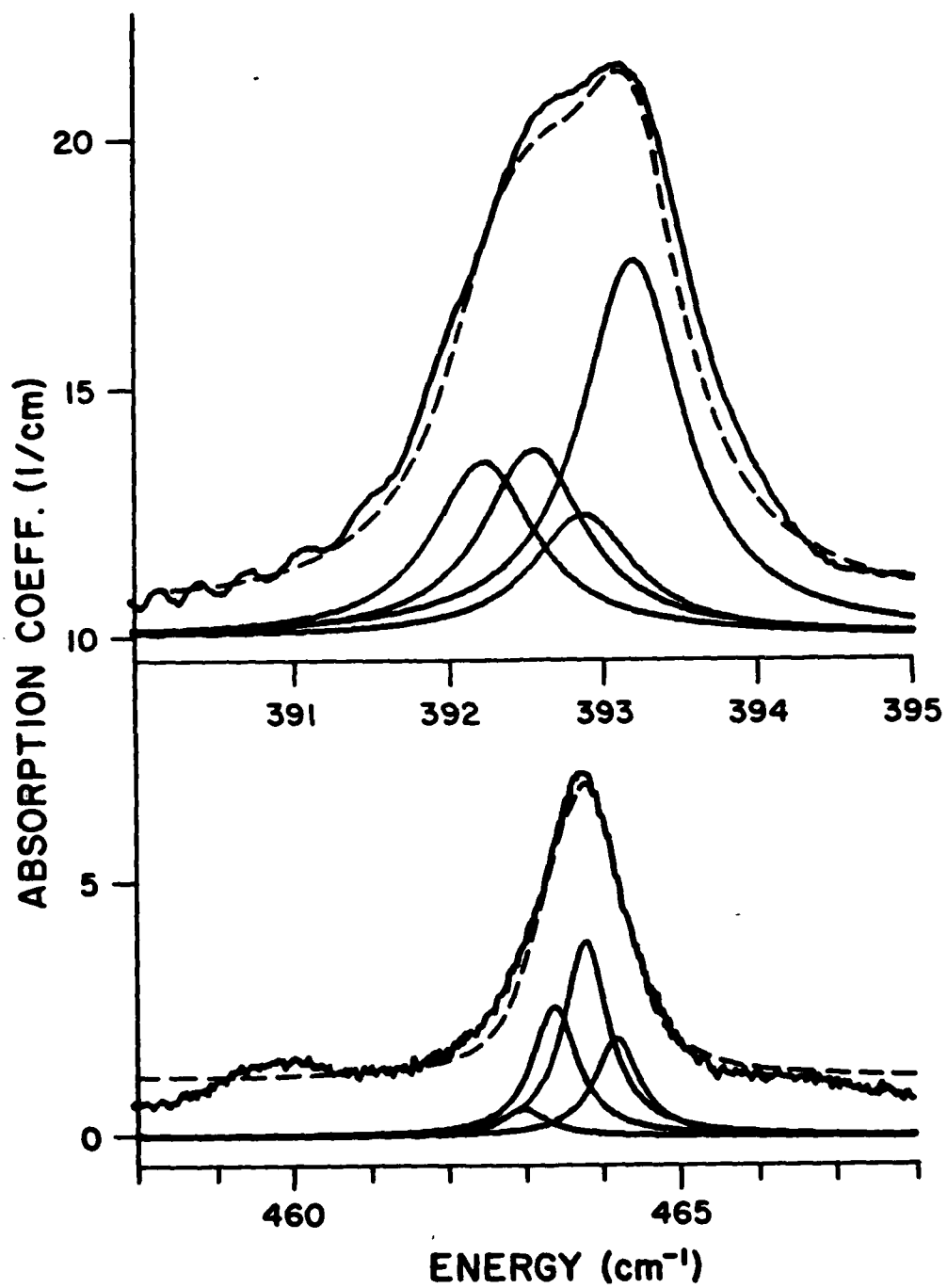
FIG 4. Fitting of pair mode absorptions to a sum of Lorentzian lineshapes for a sample with  $[\text{Si}]$  approximately  $2 \times 10^{18} \text{ cm}^{-3}$ . Relative heights are predicted utilizing the random population of nn Ga isotopes to the  $^{28}\text{Si}_{\text{As}}$  member of the dimer and assuming the FWHM for the individual lines to be that for  $\text{Si}_{\text{Ga}}$ . The sum of the individual lines, as shown below each respective absorption, are indicated by the dashed line. See text for details of the fit.

FIG 5. Infrared absorption spectra at liquid nitrogen temperature for  $A_1^+$  pair absorptions for a sample doped with both  $^{30}\text{Si}$  and  $^{28}\text{Si}$ . The various isotopic combinations for the pair absorption are indicated.

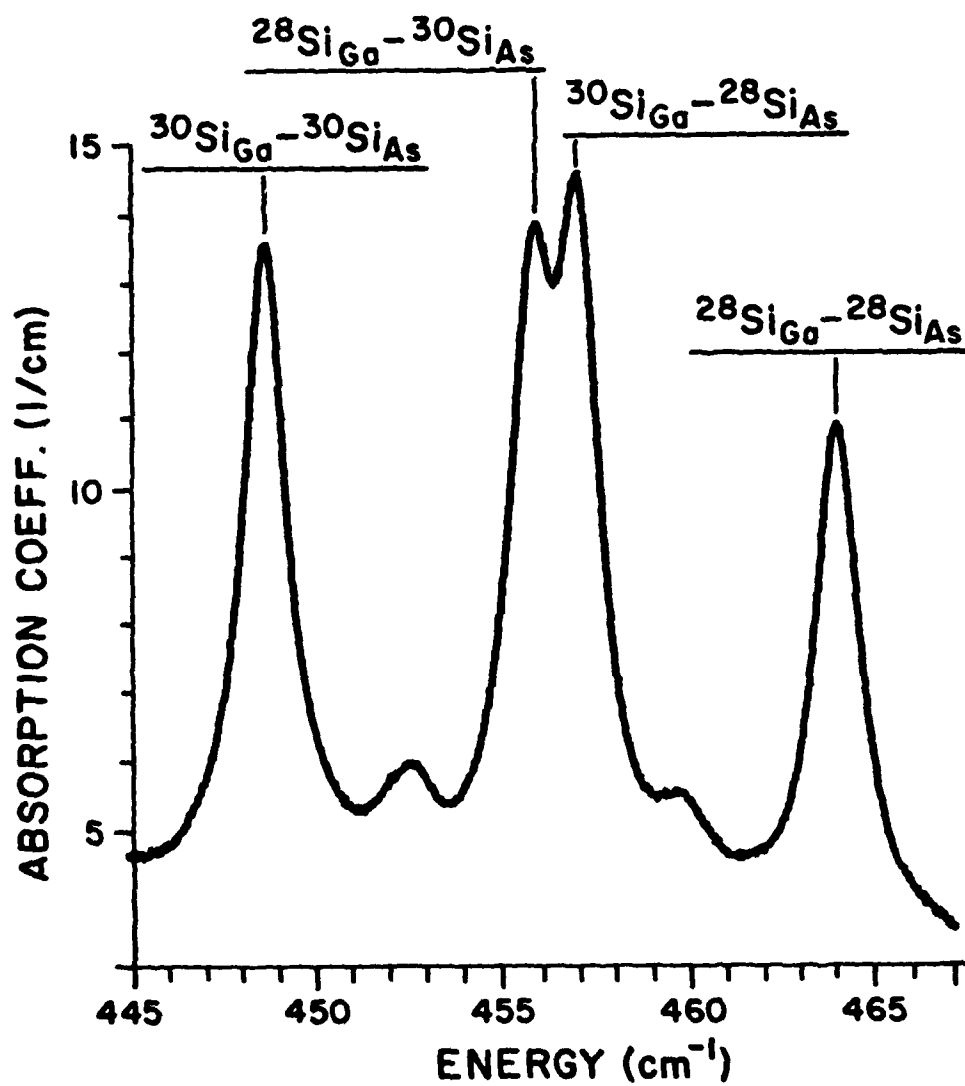












END

DATE  
FILMED

7-84

DTIC